The Influence of Sailplane Deflection on the Nominal Wake

David A. Pook[1,3], david.pook@dst.defence.gov.au
Gregory J. Seil[2,3], gregory.seil@dst.defence.gov.au
Chris Shingles [3], christopher.shingles@dst.defence.gov.au
Dev Ranmuthugala[3], dev.ranmuthugala2@dst.defence.gov.au

[1] Aerospace & Aviation, RMIT University
[2] Advanced VTOL Technologies Pty Ltd
[3] Maritime Division, Defence Science and Technology Group

ABSTRACT

This paper uses Computational Fluid Dynamics (CFD) simulations of the generic BB2 submarine geometry to investigate the effect of sailplane deflection on the nominal wake at the propeller plane. Studies of marine vehicle wakes typically consider the vessel heading straight-ahead with no deflection of the control surfaces. While this is the most-typical condition, vessels can operate for significant periods with control surfaces deflected. The wake of the control surfaces can flow downstream and alter the nominal wake seen by the propeller.

When the BB2 generic submarine geometry is simulated running straight-ahead, the wake of the sailplanes does not influence the nominal wake. However, deflection of the sailplanes can indirectly alter the nominal wake. The sailplane deflection modifies the pressure field in the vicinity of the sail, which alters the formation and downstream path of the sail-junction flow. The modification of the sail-junction flow then alters the nominal wake. Deflecting the sailplanes leading edge upwards, spreads the sail-junction flow away from the hull centreline, while an opposite deflection pulls the sail-junction flow towards the hull centreline.

INTRODUCTION

The nominal wake is defined as the flow at the propeller without including the influence of the propeller [1]. It is an important consideration when evaluating the hydrodynamics and propulsive performance of marine vessels. Adapting the propeller design for the incoming mean flow can increase the propulsive efficiency of the vessel [2, 3]. Spatial variation of the mean flow due to a non-axisymmetric hull and appendages causes unsteady loading on the propeller, creating undesired vibration. Typically, the nominal wake is evaluated for the straight-ahead condition. For surface ships, control surfaces (rudder) are often located aft of the nominal wake plane, hence they do not significantly influence the nominal wake.

The hulls of underwater vehicles are often (near) axisymmetric which minimises circumferential variation of the nominal wake. However, underwater vehicles typically

feature relatively large control surfaces and appendages (e.g. sail, casing, and sensors) upstream of the propeller. For example, the geometry of the DST Group BB2 generic submarine geometry depicted in Figure 1 features a sail, casing, four aft-control-surfaces (ACS), and two sail mounted hydroplanes (sailplanes). Seil and Anderson [4] have previously examined the effect of sail geometry on the nominal wake. Due to the large size of underwater vehicle appendages and control surfaces, their potential influence on the nominal wake is of interest.

For the BB2 geometry, a portion of each ACS is located in the hull boundary layer. Therefore, their wakes will influence the nominal wake, and their deflection will alter the nominal wake. The portion of the sail located in the hull boundary layer will also alter the nominal wake. The sail-junction (horseshoe) vortex at the sail root will also influence the nominal wake. The sailplanes are located a significant distance outside of the hull boundary layer. Hence, the wake of the sailplanes will not typically enter the propeller, except possibly during extreme manoeuvres. Therefore, it might be assumed that sailplanes will not affect the nominal wake of the BB2 generic submarine geometry.

However, this paper will demonstrate that deflection of the sailplanes indirectly alters the nominal wake by influencing the sail-junction flow. Considering the size of the sail and its location, there is potential for significant changes in the nominal wake due to sailplane deflection. The possible influence of sailplane deflection on the nominal wake has not been previously reported in literature.

DST GROUP EVOLVED GENERIC SUBMARINE GEOMETRY (BB2)

The BB2 generic submarine geometry [5] is shown in Figure 1 with a body-fitted axes system (x, y, z) at amidships and a cylindrical coordinate system (r, θ) in the nominal wake plane. The boat length from bow to stern (L) is 70.2 m for the full-scale design. The BB2 geometry is constructed from an axisymmetric hull with a length to diameter (L/D) ratio of approximately 7.3. A casing is placed on the top side of the hull, modifying the axisymmetric profile of the hull. The sail is constructed from a NACA 0021 aerofoil section. The nominal wake plane is located at 98.1% of the boat length, measured from the bow ($x/L = -0.481$). The BB2 propeller has a radius (R_p) of 2.5 m ($0.0356L$).

The sailplanes are constructed from a NACA 0015 aerofoil. The sailplanes have a fixed region (headbox) adjacent to the sail, and an outer deflecting section (see Figure 1). The sailplanes rotate (deflect) about an axis located at approximately one-third of their root chord. A positive deflection moves the leading edge up and the trailing edge down.

COMPUTATIONAL FLUID DYNAMICS MODELLING

The flow was computed using the Reynolds Averaged Navier Stokes (RANS) equations with the ANSYS Fluent 14.5 pressure based, incompressible solver, using the Shear Stress Transport (SST) $k\omega$ turbulence model, where k is the turbulent kinetic energy and ω is the specific turbulence dissipation rate. All equations were differenced using second-order schemes. Pressure-velocity couple was carried out using the SIMPLE algorithm.

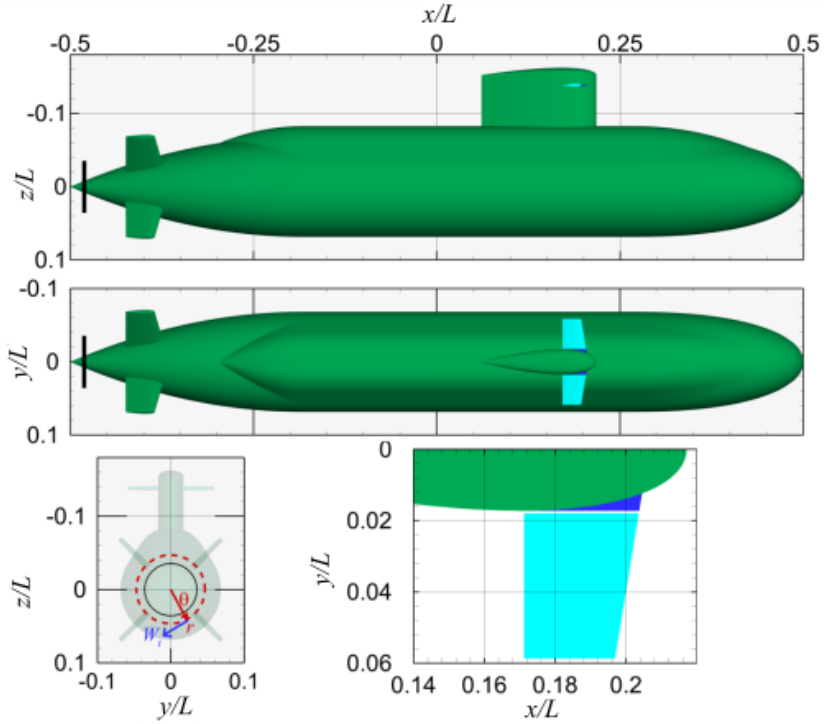

Figure 1 - DST Group BB2 generic submarine geometry, with the body-fixed coordinate system and the cylindrical coordinate system shown on the y-z plane. The outer edge of the BB2 propeller, at the nominal wake plane, is shown with the thick black vertical line. The moveable sailplane section (starboard-side) is shown in light blue. The fixed portion (headbox) of the sailplane is shown in dark blue.

The flow conditions were set to provide a Reynolds number based on length, L, of 5.2×10^6, as this Reynolds number is achievable in model-scale testing (e.g. [6]) and matches previous computational studies of the BB2 [7]. The BB2 geometry was modelled deeply submerged (no free-surface effects) and placed centrally in a rectangular domain having a length, width, height of $6.0L \times 3.0\,L \times 3.0\,L$, respectively. The distance to the domain boundary satisfies the recommended 1 to $2L$ guideline for CFD simulations of ship hull forms [8]. A uniform velocity inlet, with a velocity vector in the freestream direction, was specified on all domain boundaries. The turbulence intensity at the inlet was set as 1% and the turbulent viscosity ratio set as 10.

The grid was constructed in three distinct regions using Pointwise meshing software:

- Inner grid - containing the BB2 geometry and near flow, except the sailplanes;
- Outer grid - bounded by the outer domains and encompassing the inner grid; and
- Sailplane grid - contains on the sailplanes and near flow.

The Inner grid was a multi-block structured grid, shown in Figure 2. The cell count of the inner grid was approximately 40.2 million hexahedral cells. Seil et al. [9] performed a grid refinement study using this grid at the same Reynolds number with the same solver and settings. For straight-ahead conditions, increasing the cell count by a factor of four was found to change:

- the global resistance less than 0.06%;
- the nominal wake fraction less than 0.4%; and

- the standard deviation of the axial velocity circumferential variation (distortion coefficient) less than 3.1%.

The outer grid was also a structured grid of hexahedral cells, joined to the inner grid by a non-conformal interface boundary condition. The use of a non-conformal interface allowed a reduction in cell count in the outer grid.

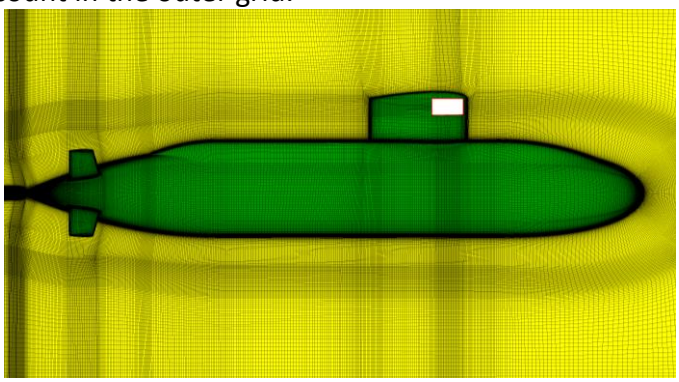

Figure 2 - Structured inner grid. The white rectangular region with a red border denotes the sailplane grid region.

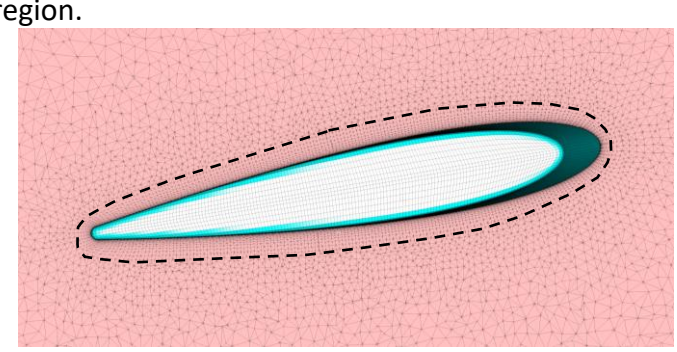

Figure 3 - Cut through a grid in the sailplane region. The dashed black line indicates the region where the Pointwise T-Rex tool recombines triangular cells to triangular prisms or hexahedra for boundary layer resolution.

The sailplane grid was unstructured and designed to simplify re-meshing of that region when the sailplane is deflected. The sailplanes were deflected to the desired angle, and the T-Rex tool within Pointwise used to grow layers of triangular prisms and hexahedra through an approximate height of the sailplane boundary layer (see Figure 3). Pyramid and tetrahedral cells then fill the sailplane grid region out to the interface boundary condition.

The wall-surfaces of the BB2 geometry were specified as non-slip walls. The first cell height was placed in the viscous sub-layer with a sub-layer scale distance (y^+) of approximately 1. The turbulence equations were integrated to the wall, i.e. no-wall function was used.

RESULTS

Overview

Figure 4 shows contours of the streamwise (x-direction) velocity component on planes normal to the hull, clipped at 95% of the freestream speed in order to represent the boundary layer thickness. The nominal wake at the propeller plane is distorted by the appendages (i.e. ACS and sail) which each create a circumferential variation (thickening/thinning) of the hull boundary layer. Each appendage creates a junction vortex

at its base in the hull boundary layer. The junction vortex is created by skewing the vorticity of the approaching hull-boundary layer around the appendage leading edge, creating a streamwise oriented vortex. The hull boundary layer thickening and thinning shown in Figure 4 can be used to trace the path of a junction vortex to the nominal wake plane.

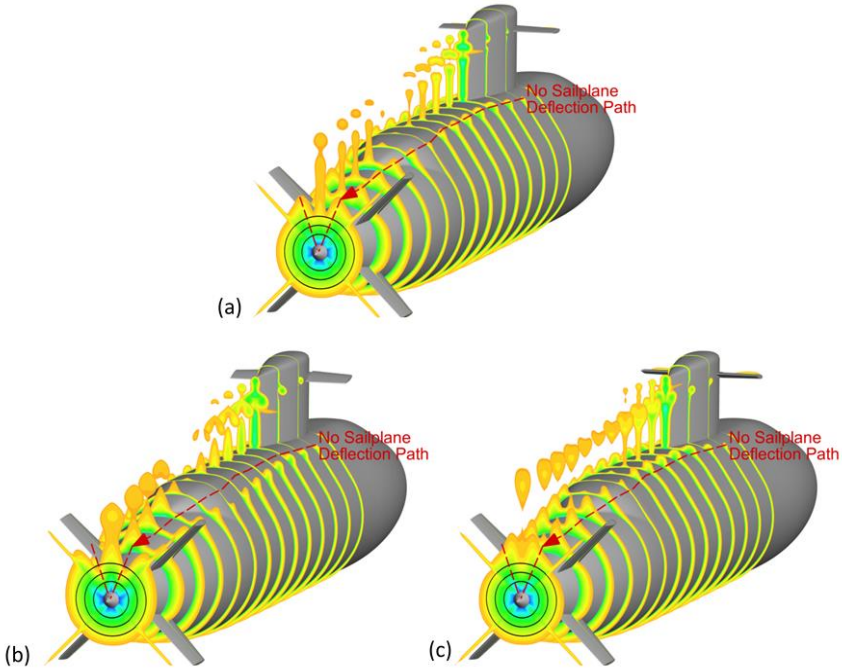

Figure 4 - Slices perpendicular to the centreline of the BB2 geometry showing contours of the streamwise velocity component. Contours cropped at 95% of the freestream speed to indicate boundary layer thickness. Sailplanes deflections: (a) undeflected; (b) leading edge up, $+10°$; (c) leading edge down, $-10°$.

Over the aft-hull section, the adverse pressure gradient compresses the streamwise oriented vorticity, possibly reducing the vorticity to a value lower than the strain. Hence Q-surfaces, typically used to identify vortices (regions where vorticity is greater than strain) cannot be used reliably to trace the sail-junction flow to the nominal wake plane.

From Figure 4, it is seen that the deflection of the sailplanes modifies the path taken by the sail-junction flow to the nominal wake plane. The red dashed line along the hull in Figure 4 indicates the path of the sail-junction flow with no sailplane deflection. Deflecting the sailplanes leading edge up (i.e. positive deflection), pushes the sail-junction flow away from the top of the hull. Conversely, deflecting the sailplane leading edge down moves the sail-junction flow towards the top of the hull.

Deflection of the sailplanes creates a `lift' force from the sailplanes, altering the pressure in the vicinity of the sail and sail-junction. Figure 5 shows contours of the pressure coefficient (C_p), defined as,

$$C_p = \frac{2(p-p_{ref})}{\rho U_\infty^2},$$

where p is the pressure, p_{ref} is a reference pressure upstream of the boat, and ρ is the fluid density. The pressure contours reveal that deflecting the leading edge of each sailplane upwards creates a higher pressure at a given distance from the sail, which pushes the sail-junction flow away from the sail as it passes downstream. Conversely, deflection

the leading edge of each sailplane downwards creates a lower pressure closer to the sail, pulling the sail-junction flow inwards.

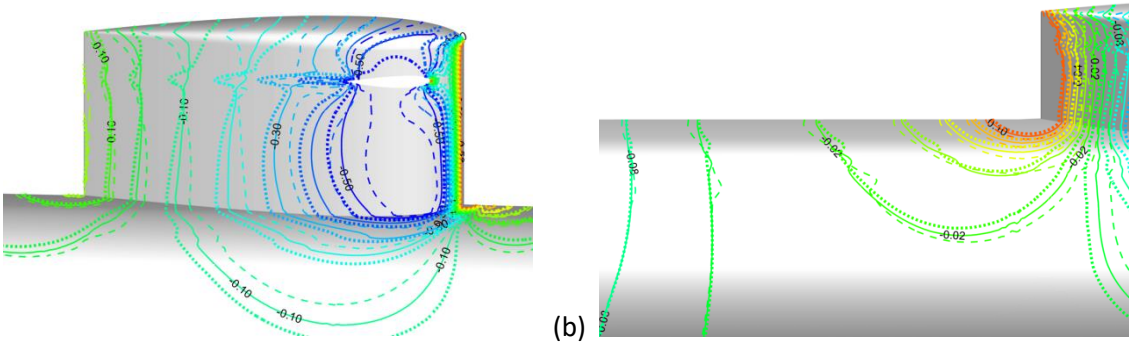

(a) (b)

Figure 5 - Contours of the pressure coefficient for the sailplanes: undeflected, solid lines; $+10^{\circ}$ deflection, dotted lines; -10° deflection, dashed lines. Views: (a) sail region (sailplane fixed root position shown in white); (b) hull downstream of the sail.

Downstream of the sail, the pressure contours for the different sailplane deflections tend to coincide (Figure 5(b)), indicating the action of the sailplane deflection on the sail-junction flow is limited to the region near the sail.

Axial Velocity

Contours of the axial velocity component (U, in the x-direction) at the nominal wake plane are shown in Figure 6 for no sailplane deflection, -15° and $+15^{\circ}$ deflection. The tip vortices created by the sailplanes bypass the BB2 propeller (propeller diameter denoted by the outer concentric black ring in Figure 6) for all sailplane deflection angles examined. The wake of the sailplanes also bypass the BB2 propeller region with a significant margin for all cases, except the $+15^{\circ}$ sailplane deflection. For this deflection, the wake of the inner sailplane approaches the propeller outer diameter. Figure 6 also shows that sailplane deflection has little effect on the nominal wake in the underside region of the hull.

Contours within the propeller radius on the topside of the BB2 in Figure 6, are clearly different for the -15° and $+15^{\circ}$ sailplane deflections. For $+15^{\circ}$ deflection, there is a significantly stronger wake region on the hull centreline behind the sail. The changing wake directly behind the sail indicates the resistance of the sail is being modified by the sailplane deflection. Higher speed flow is also brought into smaller radial distances from the hull surface on either side of the stronger centreline wake. In contrast, for -15° deflection, the wake is strengthened (i.e. lower flow speed) in this region when compared to the case of no sailplane deflection.

The differences between positive and negative sailplane deflections are highlighted in the circumferential variation of the axial velocity shown in Figure 7, at 25% and 75% of the propeller radius. The circumferential variation of the negative sailplane deflection angles is similar to that with no deflection. Negative deflection increases the variation magnitude and shifts the circumferential peak location slightly. The $+10^{\circ}$ and $+15^{\circ}$ sailplane deflections, particularly at 75% of the propeller radius, produce a very different circumferential variation due to the relatively high speed flow brought in (around $\theta \approx -70^{\circ}$ and -110°) and the stronger wake behind the line of the sail (at $\theta = -90^{\circ}$).

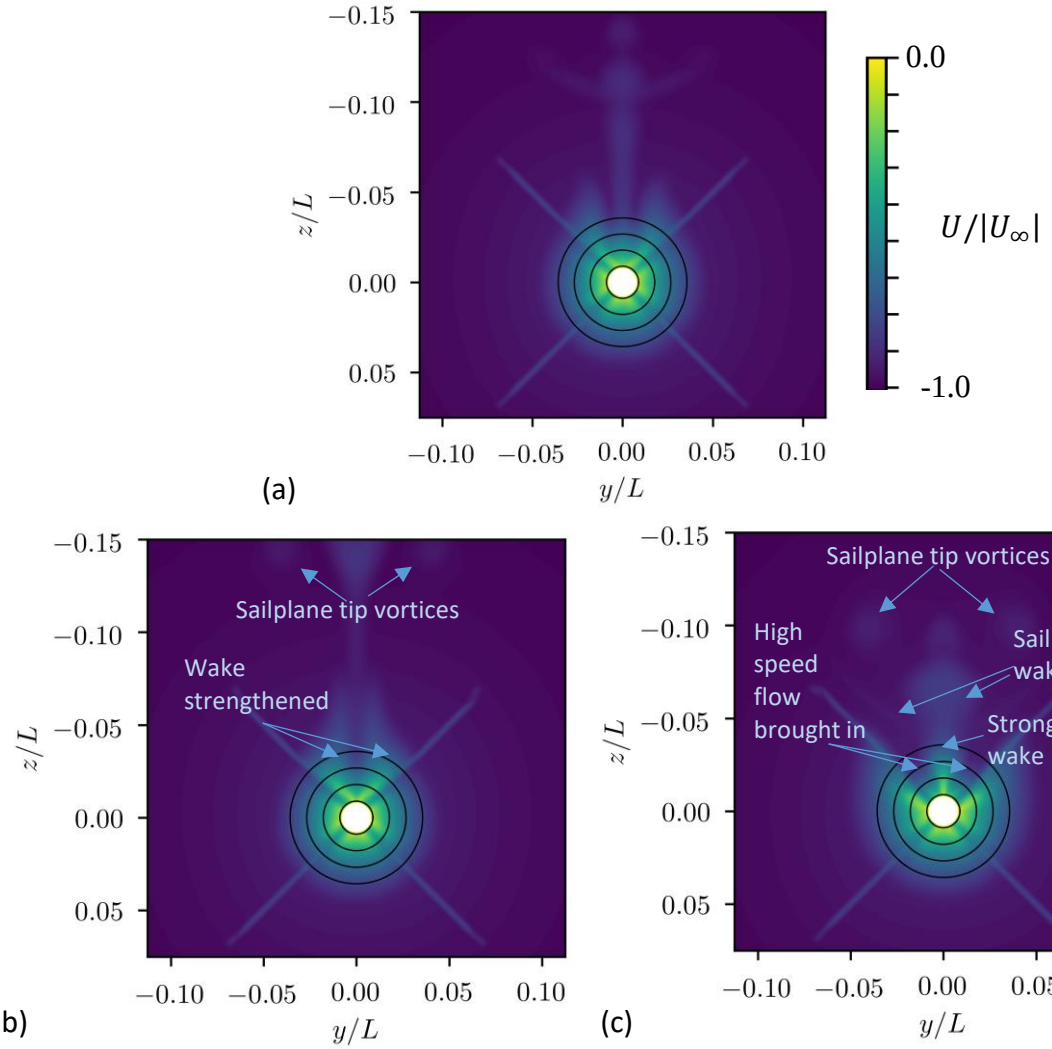

Figure 6 - Contours of the axial velocity (U) at the nominal wake plane for sailplane deflections: (a) undeflected; (b) $-15°$; (c) $+15°$. The black concentric rings are at a radius of $0.25R_p$, $0.5R_p$, $0.75R_p$ and $1.0R_p$.

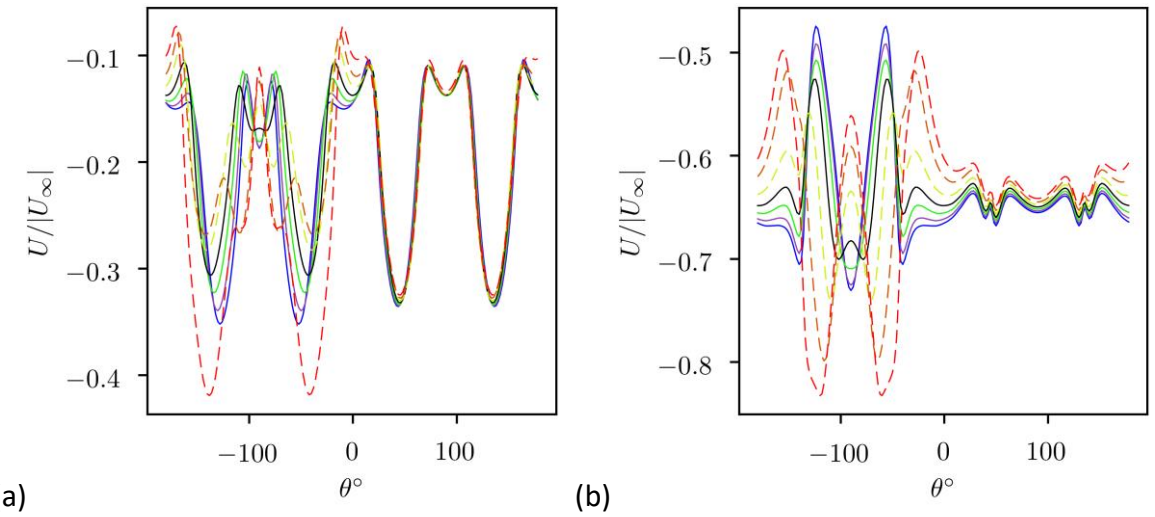

Figure 7 - Circumferential variation of the axial velocity at the propeller plane at a radius of: (a) $0.25R_p$; (b) $0.75R_p$. Sailplane deflection lines: undeflected, ——; $-5°$, ——; $-10°$, ——; $-15°$, ——; $+5°$, - - -; $+10°$, - - -; $+15°$, - - -.. Sail located at $\theta = -90°$.

Radial Variation

The radial variation of the circumferential mean (μ) of the axial velocity at the nominal wake plane is shown in Figure 8(a). The mean axial velocity is altered slightly below 40% of the propeller radius, particularly for the $+15°$ sailplane deflection. All sailplane deflections increase the net mass flow available to the propeller. The circumferential mean of the turbulent kinetic energy is shown in Figure 8(b). Deflection of the sailplane in either direction typically increases the turbulent kinetic energy over approximately 80% of the propeller radius.

The radial variation of the standard deviation in the circumferential direction (σ) of the axial velocity (distortion coefficient [10]) and the tangential velocity (W_t) are shown in Figure 8(c) and (d) respectively. The standard deviation gives a measure of the circumferential variation. Deflection of the sailplane leading edge by $+10°$ and $+15°$ significantly increases the axial velocity variation over most of the propeller radius, more than doubling it at some radii. The standard deviation of the tangential velocity component is also increased substantially.

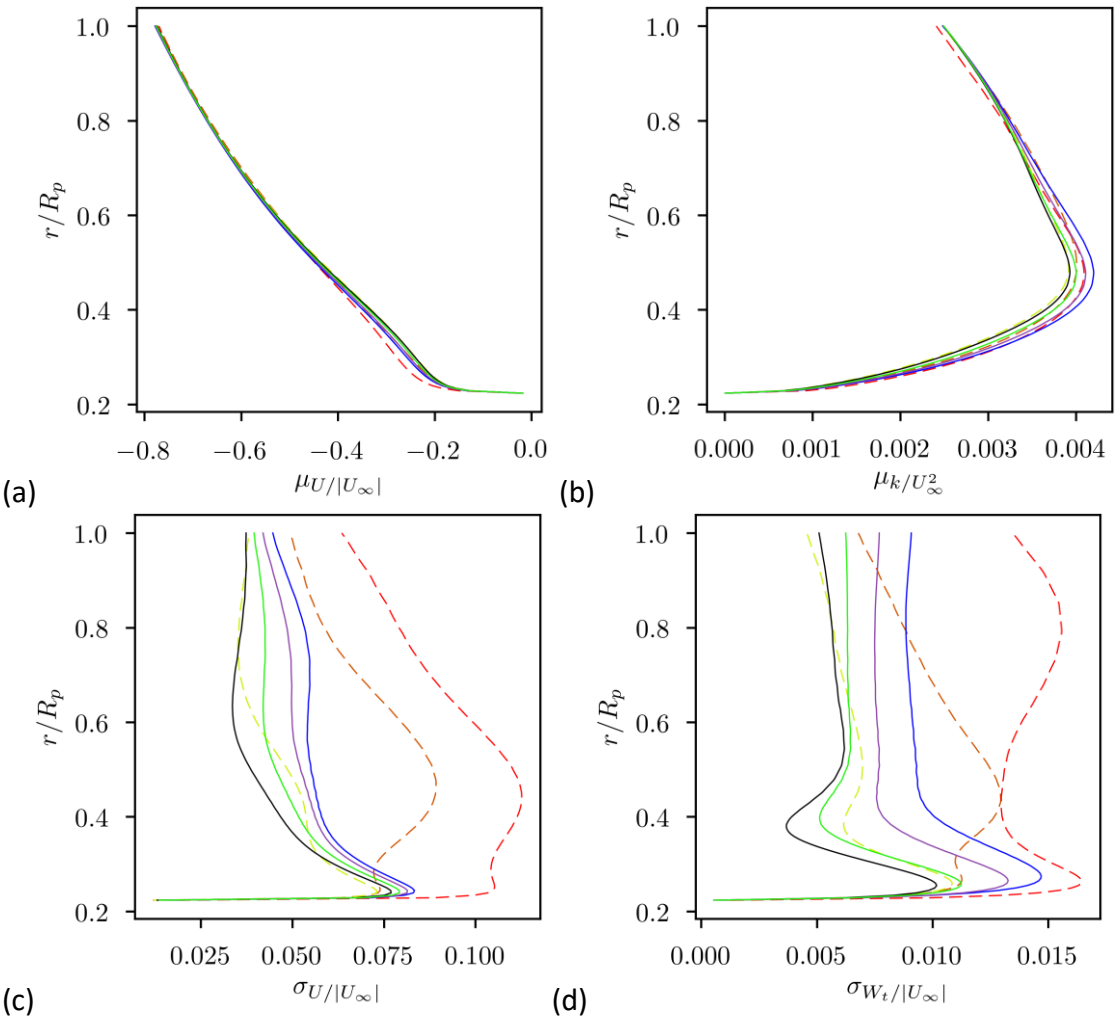

Figure 8 - Radial variation of the circumferential: (a) mean axial velocity; (b) mean turbulent kinetic energy; (c) standard deviation of the axial velocity; (d) standard deviation of the tangential velocity. Sailplane deflection lines: undeflected, ——; $-5°$, ——; $-10°$, ——; $-15°$, ——; $+5°$, - - - -; $+10°$, - - - -; $+15°$, - - - -.

DISCUSSION

The results presented show that for the BB2 generic submarine geometry, deflection of the sailplanes can significantly alter the mean flow spatial variation of the nominal wake. Deflecting the leading edge upwards (positive sailplane deflection) had a greater effect on the nominal wake than downwards deflection. The nominal wake variation is due to the pressure field created by the sailplane deflection altering the sail-junction flow as it passes around the sail. As this is an indirect mechanism, the potential for sailplane deflection to alter the nominal wake will be design dependant. Reduction of the sail-junction vortex through improved sail design, filleting, etc. [11] might minimise the effect of sailplane deflection on the nominal wake. However, any geometry contouring in the sail region to minimise the sail-hull junction vortex will still be affected by sailplane deflection. In the absence of a significant sail-junction flow, sailplane deflection might still induce a lateral pressure gradient in the hull boundary layer that could create a local thickening/thinning that would flow downstream to the propeller. The sailplane geometry, and its relative distance to the sail-junction flow, will also alter the significance of any sailplane deflection.

The hull and casing shape in the vicinity of the sail, and downstream of the sail to the propeller, is a significant parameter that will affect the significance of sailplane deflection on the nominal wake. The BB2 geometry has a `flat' top casing in the vicinity of the sail. Thus, the sail-junction flow passes on a near horizontal surface and sailplane deflection shifts the junction flow inwards or outwards. However, hull shapes can be near axisymmetric or `boxy', i.e. with a near oval/square cross section. On an axisymmetric hull, deflection of the sailplane would be expected to shift the junction flow in/out in relation to the sailplane deflection. On a `boxy' hull, the junction flow could be pushed over (or brought back from) the edge of the casing, resulting in a strong non-linear relationship with sailplane deflection. The lack of a horizontal surface past the sail's maximum thickness might also alter the sailplane affect on the sail-hull junction vortex path. The arrangement of the ACS will also change the effect of the sailplane deflection if the sail-junction disturbance is moved near an ACS.

The CFD techniques used to model the BB2 geometry (e.g. SST $k\omega$ turbulence model) in this paper are known to have limitations accurately predicting junction flows (see [12] for a summary). However, the mechanism by which the sailplane can alter the nominal wake is captured by the modelling presented in this paper, and thus serves as a demonstration of the expected effects due to sailplane deflection. The results presented should not be interpreted as a prediction of absolute values. However, Chase [13] found predictions of the Suboff submarine geometry nominal wake, circumferential mean axial velocity, calculated using the using the SST $k\omega$ turbulence model (straight-ahead, Re$= 12 \times 10^6$) were within 3.85% of the experimental measurements made by Crook [14]. The nominal wake distortion due to the sail-junction wake was also consistent with measurements. Hence, the computations presented in this paper for the BB2 geometry are likely a reasonable prediction.

The simulations in this paper considered a steady flow with turbulent fluctuations (Reynolds stresses). The real junction flow to the propeller will possibly 'wander', particularly if it is pushed onto a highly curved region like the top edge of the BB2 casing. The simulations also do not model the transient effect on the BB2 motion due to sailplane

deflection, nor the new steady-state condition the BB2 would achieve (i.e. relative angle of attack, vertical velocity component). These complications would alter the predicted effect of sailplane deflection on the nominal wake.

The results presented are for a model-scale Reynolds number. From model-scale to full-scale, the wake-fraction is known to change due to the relative thinning of the hull boundary layer. The sail-junction flow will still be present in the hull boundary layer at full-scale Reynolds numbers, although its characteristics (e.g. location, strength, streamwise decay) may change with Reynolds number. Thus, deflection of the sailplanes, which alters the sail-junction flow by changing the local pressure field, will still influence the sail-junction flow at full-scale Reynolds numbers. However, the sensitivity of the nominal wake to sailplane defection at full-scale Reynolds numbers requires further assessment.

CONCLUSION

Deflection of the BB2 generic submarine geometry sailplanes was shown to alter the path of the sail-junction vortex and modify the nominal wake. This effect was demonstrated using RANS-based CFD modelling. Deflecting the sailplane leading edge upwards pushed the sail-junction flow outwards (away from the top of the hull). A stronger wake on the hull centreline was also created. Deflecting the sailplane leading edge downwards pulled the sail-junction flow inwards, towards the top of the hull. For the BB2 generic submarine geometry and a given sailplane deflection angle, deflecting the leading edge of the sailplanes upwards (positive sailplane deflection) had a larger influence on the nominal wake.

REFERENCES

1. Carlton, J., *Marine Propellers and Propulsion*. 2nd ed. 2007: Butterworth-Heinemann.
2. Renilson, M., *Submarine Hydrodynamics*. 2nd ed. 2018: Springer.
3. ITTC, *The Specialist Committee on Scaling of Wake Field - Final Report and Recommendations to the 26th ITTC*. in *Proceedings of 26th ITTC*. 2011. Rio de Janeiro, Brazil.
4. Seil, G.J. and Anderson, B., *A Comparison of Submarine Fin Geometry on the Performance of a Generic Submarine*, in *Pacific 2012 International Maritime Conference*. 2012: Sydney, Australia.
5. Overpelt, B., Nienhuis, B., and Anderson, B., *Free Running Manoeuvring Model Tests on a Modern Generic SSK Class Submarine (BB2)*, in *Pacific International Maritime Conference*. 2015: Sydney, Australia.
6. Pook, D.A., Clarke, D.B., Jones, M., Quick, H., and Ranmuthugala, D., *RANS based CFD Prediction of Submarine Hydrodynamic Loads*, in *21st Australasian Fluid Mechanics Conference*. 2018: Adelaide, Australia.
7. Seil, G.J., Pook, D.A., Nguyen, M.C., and Leong, Z.Q., *The Influence of Appendages and their Stall on Submarine Hydrodynamic Loads*, in *PACIFIC 2017 International Maritime Conference*. 2017: Sydney, Australia.
8. ITTC, Recommended Procedures and Guidelines *Practical Guidelines for Ship CFD Applications,* **7.5-03-02-03 Rev. 01**, 2011
9. Seil, G.J., Nguyen, M.C., Pook, D.A., and Leong, Z.Q., *CFD Study of the Hydrodynamics of the Evolved DST Group Generic Submarine (BB2)*. 2019, Defence Science & Technology Group.

10. Seil, G.J., Nguyen, M.C., and Pook, D.A., *CFD Study of the KJ01 Submarine with Validation Against Wind Tunnel Measurements (FOUO, AUSTEO)*. 2019, Defence Science & Technology Group.
11. Toxopeus, S., Kuin, R., Kerkvliet, M., Hoeigmakers, H., and Nienhuis, B., *Improvement of Resistance and Wake Field of an Underwater Vehicle by Optimising the Fin-Body Junction Flow with CFD*, in *Proceedings of ASME 33rd International Conference on Ocean, Offshore and Arctic Engineering*. 2014: San Francisco, California.
12. Gand, F., Decl, S., Brunet, V., and Sagaut, P., *Flow dynamics past a simplified wing body junction.* Physics of Fluids, 2010. **22**: p. 115111.
13. Chase, N., *Simulations of the DARPA Suboff submarine including self-propulsion with the E1619 propeller*, 2012, Thesis, The University of Iowa
14. Crook, B., *Resistance for DARPA Suboff as Represented by Model 5470*, 1990, David Taylor Research Center, DRTC/SHD-1298-07